

Sparse Bayesian Learning with Diagonal Quasi-Newton Method for Large Scale Classification

Jiahua Luo, Chi-Man Vong, Chi-Man Wong, Jie Du

Abstract—Sparse Bayesian Learning (SBL) constructs an extremely sparse probabilistic model with very competitive generalization. However, SBL needs to invert a big covariance matrix with complexity $O(M^3)$ (M : feature size) for updating the regularization priors, making it difficult for practical use. There are three issues in SBL: 1) Inverting the covariance matrix may obtain singular solutions in some cases, which hinders SBL from convergence; 2) Poor scalability to problems with high dimensional feature space or large data size; 3) SBL easily suffers from memory overflow for large-scale data. This paper addresses these issues with a newly proposed diagonal Quasi-Newton (DQN) method for SBL called DQN-SBL where the inversion of big covariance matrix is ignored so that the complexity and memory storage are reduced to $O(M)$. The DQN-SBL is thoroughly evaluated on non-linear classifiers and linear feature selection using various benchmark datasets of different sizes. Experimental results verify that DQN-SBL receives competitive generalization with a very sparse model and scales well to large-scale problems.

Index term—diagonal Quasi-newton method, Sparse Bayesian Learning, large-scale problems, Sparse model

I. INTRODUCTION

Currently, research on deep learning methods is prevalent in the machine learning community. However, it requires rather large-scale data for training a deep model and lacks interpretability for the model structure. In many applications, such as antispam, fault diagnosis, on-board controls, robot devices and other Internet of Things (IoT) applications with small training data or limited computational resources (CPU or memory), a non-deep learning method with competitive accuracy and relatively compact model is preferred.

Traditional machine learning methods, like Logistic Regression (LR) [1-2], Support Vector Machine (SVM) [3-4], Sparse Bayesian models (SBL) [5-6], and so on with their variants gain lots of attraction in recent years in both academic and industry for the problems with small training data. Such sparse learning methods balance the model sparsity and generalization.

LR with ℓ_1 -penalty is very suitable for dealing with high-

dimensional feature space problems and is widely adopted in various industries. LR provides a sparse and interpretable model structure and good generalization with probabilistic outputs. Nevertheless, it depends on an exhaustive search for the regularization parameters by cross-validation. SVM builds classifiers from kernel space by maximizing the margin hyperplane, achieving sparsity with few support vectors (samples). SVM provides state-of-the-art accuracy for small-data problems. Since its model size is proportional to the number of training data, SVM usually obtains a corpulent model, yet without probabilistic prediction. Like LR, SVM relies on an exhaustive grid search of the hyperparameters (penalty and kernel radius).

SBL is a probabilistic model for regression and classification. When modeling classification problems, SBL is built on the likelihood of training data. It can also be treated as a penalized LR model except that the regularization parameters in SBL are automatically determined by the training data, which avoids manual selection for hyperparameters. The regularization hyperparameters are assumed with Gaussian distributions, namely automatic relevance determination (ARD) prior [5], which provides competitive accuracy with a highly sparse model without significant deterioration of generalization. This advantage makes SBL very suitable and widely used for compressive sensing and recovery [7-10,28].

In many industrial devices with limited computational resources, training time is not the main concern but the fast execution time with a tiny and high precision model. SBL is well suited for such memory-critical and/or timely-responsive applications. Based on the SBL framework, many variants were proposed, amongst which the representatives are Relevance vector machine (RVM) [5] and Sparse Bayesian extreme learning machine (SBELM) [11-12] that provide the most competitive precision and sparsity. The process of RVM is identical to SVM by mapping the input features to a kernel space but employing SBL to carry out the model training. SBELM is a MLP alike model whose feature is randomly mapped to the hidden layer and SBL is employed to select the

This work is funded by The Science and Technology Development Fund, Macao SAR (File No: 0112/2020/A). This work has been uploaded to arxiv <https://arxiv.org/abs/2107.08195>.

J. Luo is with the Department of Computer and Information Science, University of Macau, Macao SAR, China. He received his Phd degree from university of Macau in 2021. (e-mail: luojiahua@163.com).

C.-M. Vong is with the Department of Computer and Information Science, University of Macau, Macao SAR, China (e-mail: cmvong@um.edu.mo).

C.-M. Wong is with the Department of Computer and Information Science, University of Macau, Macao SAR, China (e-mail: yc17417@um.edu.mo).

J. Du is with the School of Biomedical Engineering, Health Science Center, Shenzhen University, Shenzhen, China (e-mail: dujie@szu.edu.cn)

most relevant hidden nodes, and thus achieving sparsity. SBELM achieves comparative accuracy with shorter training time than RVM and is insensitive to the training data size N , resolving the bottleneck of RVM in modeling problems with large training instances.

Generally, the learning of SBL contains two main stages [5]:

(1) **MAP-Stage**: Maximize the likelihood function (1) to estimate \mathbf{w} , also interpreted as *maximum a posteriori* (MAP).

$$\hat{\mathbf{w}} = \arg \max_{\mathbf{w}} [\ell(\mathbf{w}) + \log p(\mathbf{w})] \quad (1)$$

2) **A-Stage**: Update the ARD prior α using the diagonal elements of the covariance matrix (Hessian matrix inversion) calculated at the **MAP-Stage**.

Since SBL contains the colossal covariance matrix inversion with complexity $O(M^3)$ (M : feature dimension), it may incur the memory overflow issue, making poor scalability to large problems. On the other hand, RVM and its variant face the bottleneck that it could not handle a large number N of training data due to the heavy complexity $O(N^3)$. SBELM resolves this drawback by mapping the input features to hidden neurons. As SBELM requires a large number of neurons for high generalization, it becomes a challenging issue for SBELM to handle high dimensional problems.

Some works [7-10] effectively address this issue in compressive sensing, where it is treated as a regression problem and employs SBL to estimate the signal noises by selecting the most representative signals (i.e., a subset of relevant basis functions in RVM) to compress the original signals. As the training data size is relatively small in this area, these works aim to reducing the complexity of converting the covariance matrix inversion from $O(N^3)$ to $O(N^2)$ (here N denotes the size of training data in RVM) by approximating a lower bound for the MAP using Bayesian variational inference [13,14]. Other works [15-19] using SBL for classification or feature selection are mainly for small problems. Some of which [17,19] adopt a greedy strategy to sequentially add or delete the basis to/from the marginal likelihood maximization under the RVM framework. To some extent, such greedy sequential algorithms extend SBL for relatively large problems with a sacrifice of accuracy.

In past years, Quasi-newton methods like LBFGS, Trust Region method achieve success in building LR and SVM for large-scale machine learning [1, 26, 27]. Intuitively, such methods are appropriate for the MAP in SBL. However, the critical issue in SBL is that it relies on the diagonal elements in the covariance inverse matrix (the inverse Hessian matrix) achieved at the **MAP-stage** to update the ARD prior. Such inversion takes computational complexity $O(M^3)$ and storage memory $O(M^2)$. This heavy burden becomes an obstacle for SBL to scale to large problems. For this consideration, most gradient-based solvers and Quasi-newton methods without explicitly calculating the inverse Hessian matrix are not appropriate for SBL, and therefore limiting the usage of the classical SBL and its variants for large-scale machine learning problems. In this paper, we develop a diagonal Quasi-Newton (DQN) method for estimating \mathbf{w} and approximate the inverse Hessian matrix at the **MAP-Stage** for SBL (called DQN-SBL).

In DQN-SBL, the covariance matrix inversion is ignored but approximated by a diagonal positive-definite matrix, alongside estimating \mathbf{w} . Analogous to the classical SBL, the diagonal elements are alternately employed to update the regularization priors. The contribution of this paper is summarized as follows:

- 1) The computational and storage complexity in DQN-SBL is linear to the feature dimension M (or N : the number of training data in RVMs). The complexity is reduced from $O(M^3)$ to $O(M)$, avoiding the memory overflow issue for large problems.
- 2) DQN-SBL can also be used for large-scale feature selection problems with millions to billions of feature dimensions. While SBL is not suitable for such applications.

The organization of this paper: Section II provides brief reviews of SBL. DQN-SBL is proposed using the DQN method in Section III. Experimental evaluations for our proposed algorithms are arranged in Section IV. Finally, we conclude our work in Section V.

II. SHORT REVIEW OF SBL

Given a set of N training data $\mathcal{D} = (\mathbf{x}_i, t_i)$, $i = 1$ to N with each \mathbf{x}_i an M -dimensional vector and t_i a binary output. In the SBL framework, the output t is assumed with an independent Bernoulli distribution $p(t|\mathbf{x})$. Thus, for all training instances, the likelihood is the following probabilistic product

$$p(t|\mathbf{w}, \mathbf{x}) = \prod_{i=1}^N \sigma\{\mathcal{Y}(\mathbf{x}_i; \mathbf{w})\}^{t_i} [1 - \sigma\{\mathcal{Y}(\mathbf{x}_i; \mathbf{w})\}]^{1-t_i} \quad (2)$$

where the $\sigma(\cdot)$ is the sigmoid activation, $\sigma\{\mathcal{Y}(\mathbf{x}; \mathbf{w})\} = 1/(1 + e^{-\mathbf{x}^T \mathbf{w}})$. For the sake of simplicity, we denote $y = \sigma\{\mathcal{Y}(\mathbf{x}; \mathbf{w})\}$ hereafter and $\mathbf{w} = (w_0, \dots, w_M)^T$ the associated training weights. Besides, in SBL, each output weight $w_k \in \mathbf{w}$ ($k = 0, \dots, M$) is assumed with an independent zero-mean Gaussian distribution on an automatic relevance determination (ARD) hyperparameter α_k [5] such that

$$p(w_k|\alpha_k) = \mathcal{N}(w_k|0, \alpha_k^{-1}) \quad (3)$$

Then the distribution over \mathbf{w} is the product of $p(w_k|\alpha_k)$, which can be formulated as

$$p(\mathbf{w}|\alpha) = \prod_{k=0}^M \frac{\alpha_k}{\sqrt{2\pi}} \exp\left(-\frac{\alpha_k w_k^2}{2}\right) \quad (4)$$

Where $\alpha = [\alpha_0, \dots, \alpha_M]^T$. Every α_k is a positive value, the variance of w_k and governs its complexity. Each α_k can be further assumed with a Gamma distribution [5], whose parameters are usually set to zeros. The estimation of \mathbf{w} in SBL is to approximate a Gaussian distribution over \mathbf{w} . Since this is an essential procedure for integrating the probabilistic marginal distribution for $p(\mathbf{t}|\alpha, \mathbf{X}) = \int p(\mathbf{t}|\mathbf{w}, \mathbf{X})p(\mathbf{w}|\alpha) d\mathbf{w}$ by approximating a Gaussian

$$p(\mathbf{w}|\mathbf{t}, \alpha, \mathbf{X}) = \frac{p(\mathbf{t}|\mathbf{w}, \mathbf{X})p(\mathbf{w}|\alpha)}{p(\mathbf{t}|\alpha, \mathbf{X})} \propto \mathcal{N}(\hat{\mathbf{w}}, \Sigma) \quad (5)$$

The Gaussian approximation is achieved by a Taylor expansion on the logarithmic $\log\{p(\mathbf{t}|\mathbf{w}, \mathbf{X})p(\mathbf{w}|\alpha)\}$. The covariance

Σ and the Gaussian mode $\hat{\mathbf{w}}$ are attained by setting $\nabla_{\mathbf{w}} \log\{p(\mathbf{t}|\mathbf{w}, \mathbf{X})p(\mathbf{w}|\boldsymbol{\alpha})\}|_{\hat{\mathbf{w}}} = 0$, that

$$\hat{\mathbf{w}} = \boldsymbol{\beta}\Sigma\mathbf{x}\mathbf{t} \quad (6)$$

$$\Sigma = (\mathbf{X}^T \boldsymbol{\beta}\mathbf{X} + \mathbf{A})^{-1} \quad (7)$$

Where $y_i = \sigma[\mathcal{Y}(\mathbf{x}_i; \mathbf{w})]$ and \mathbf{A} is a diagonal matrix $\mathbf{A} = \text{diag}(\boldsymbol{\alpha})$. $\boldsymbol{\beta}$ is a $N \times N$ diagonal matrix with element $\beta_{ii} = y_i(1 - y_i)$, here $\mathbf{t} = [t_1, \dots, t_N]$ denotes the vector of N true outputs in the training dataset. After approximated by the Gaussian mode $\hat{\mathbf{w}}$ and covariance matrix Σ , the integral for $p(\mathbf{t}|\boldsymbol{\alpha}, \mathbf{x})$ becomes tractable. SBL estimates the unknown parameters $\boldsymbol{\alpha}$ by setting the $\nabla_{\boldsymbol{\alpha}} \log p(\mathbf{t}|\boldsymbol{\alpha}, \mathbf{x}) = 0$.

$$\begin{aligned} \frac{\nabla_{\alpha_k} \log p(\mathbf{t}|\boldsymbol{\alpha}, \mathbf{x})}{\partial \alpha_k} &= \frac{1}{2\alpha_k} - \frac{1}{2} \Sigma_{kk} - \frac{1}{2} \hat{w}_k^2 = 0 \\ \Rightarrow \alpha_k^{new} &= \frac{1 - \alpha_k \Sigma_{kk}}{\hat{w}_k^2} \end{aligned} \quad (8)$$

Using (6), (7) and (8), the output weights w_k and its associated hyperparameters α_k can be iteratively determined. Refer to the ARD [5-6], during the iteration, many α_k can be tuned to infinity such that their associated w_k becomes zero. Since α_k is inversely proportional to the output weight \hat{w}_k with (3), such weights are not updated in the subsequent iterations, which results in a highly sparse model.

III. THE PROPOSED DQN-SBL

A. Another perspective to the MAP function

Since $p(\mathbf{w}|\mathbf{t}, \boldsymbol{\alpha}, \mathbf{X}) \propto p(\mathbf{t}|\mathbf{w}, \mathbf{X})p(\mathbf{w}|\boldsymbol{\alpha})$, it is equivalent to finding the maximum, or name maximum a posterior (MAP) of $p(\mathbf{w}|\mathbf{t}, \boldsymbol{\alpha}, \mathbf{X})$ over \mathbf{w} ,

$$\begin{aligned} \log\{p(\mathbf{t}|\mathbf{w}, \mathbf{X})p(\mathbf{w}|\boldsymbol{\alpha})\} &= \\ \sum_{i=1}^N \{t_i \log y_i + (1 - t_i) \log(1 - y_i)\} - \frac{1}{2} \mathbf{w}^T \mathbf{A} \mathbf{w} \end{aligned} \quad (10)$$

Let

$$L(\mathbf{w}) = -\log\{p(\mathbf{t}|\mathbf{w}, \mathbf{X})p(\mathbf{w}|\boldsymbol{\alpha})\} \quad (11)$$

$\hat{\mathbf{w}}$ is estimated by

$$\hat{\mathbf{w}} = \arg \min_{\mathbf{w}} L(\mathbf{w}) \quad (12)$$

The Gaussian mean $\hat{\mathbf{w}}$ and variance matrix Σ are achieved using (12), here Σ is the inverse Hessian matrix at its minimum.

Theorem 1 *The function $L(\mathbf{w})$ by (11) is convex and globally converges to the unique minimum.*

Proof. We calculate out the Hessian matrix of $L(\mathbf{w})$

$$\nabla_{\mathbf{w}}^2 L(\mathbf{w}) = \mathbf{X}^T \boldsymbol{\beta}\mathbf{X} + \mathbf{A}$$

as each diagonal value of $\boldsymbol{\beta}$, $\beta_{ii} = y_i(1 - y_i) > 0$

and the diagonal value of \mathbf{A} , $\alpha_k > 0$

So, the Hessian matrix is positive definite

$$\nabla_{\mathbf{w}}^2 L(\mathbf{w}) > 0$$

Therefore, **Theorem 1** holds. Many gradient-based optimizers are appropriate for (12) to find the minimum.

B. A Diagonal QN method to SBL(DQN-SBL)

Previously, SBL and its variants need to calculate out the inverse Hessian matrix Σ , this includes utilizing a second-order Newton-Raphson method for the MAP function [5,11,12]. However, there exists two issues in such method. On the one hand, in some particular cases, Σ might be ill-conditioned [22] which leads to the training failure, i.e., the optimal weight \mathbf{w} cannot be found. On the other hand, the complexity of calculating the inverse Hessian matrix is $O(M^3)$. It may result to memory-overflow for high-dimensional or big data problems, yet it cannot be implemented in parallel for the circumstance with huge training data size. Due to this issue, most SBL and its variants only address small problems.

In convex optimization, an alternative is using a Quasi-newton method to approximate the Hessian matrix. In literature, the most representatives are BFGS and L-BFGS [20]. L-BFGS is not suitable in SBL, as it is without an explicit Hessian matrix, which is essential for updating the regularization parameter $\boldsymbol{\alpha}$ using (8).

In BFGS, $L(\mathbf{w})$ is approximated by a second-order Taylor expansion. For any \mathbf{w} , define $\boldsymbol{\delta}_m = \mathbf{w}_{m+1} - \mathbf{w}_m$, and $\boldsymbol{\gamma}_m = \nabla L(\mathbf{w}_{m+1}) - \nabla L(\mathbf{w}_m)$ at m^{th} iteration, The Hessian matrix is approximated with a full positive definite \mathbf{H} achieved by solving

$$\mathbf{H}_{m+1} = \underset{\mathbf{H}}{\text{argmin}} \|\mathbf{H} - \mathbf{H}_m\|_{\mathbf{w}}$$

$$s. t. \mathbf{H} = \mathbf{H}^T \text{ and } \mathbf{H}\boldsymbol{\delta}_m = \boldsymbol{\gamma}_m$$

\mathbf{H} is updated by the following formula

$$\mathbf{H}_{m+1} = \mathbf{H}_m + \frac{\boldsymbol{\gamma}_m \boldsymbol{\gamma}_m^T}{\boldsymbol{\gamma}_m^T \boldsymbol{\delta}_m} - \frac{\mathbf{H}_m \boldsymbol{\delta}_m \boldsymbol{\delta}_m^T \mathbf{H}_m}{\boldsymbol{\delta}_m^T \mathbf{H}_m \boldsymbol{\delta}_m} \quad (13)$$

However, it is computational expensive to approximate and store such a $M \times M$ full matrix \mathbf{H} for high dimensional problems with computational and storage complexity $O(M^2)$. When M amplifies in large problems, the storage and update of \mathbf{B} become intractable.

In this subsection, we develop a diagonal Quasi-newton (DQN) method for approximating Σ for $L(\mathbf{w})$. In this methodology, Σ is approximated by a diagonal matrix \mathbf{B} instead of using a full matrix. \mathbf{B} shall satisfies the weak secant equation [21].

Derived from the BFGS formula (13), we here develop the diagonal updating type for the BFGS formula. Instead of approximating the Hessian matrix, we develop its inverse type \mathbf{B} . Due to the fact that,

$$\mathbf{B}_{m+1}^{-1} = \text{diag}[(\mathbf{B}_{m+1}^{(1)})^{-1}, (\mathbf{B}_{m+1}^{(2)})^{-1} \dots (\mathbf{B}_{m+1}^{(k)})^{-1}]$$

By (13), we have

$$\mathbf{B}_{m+1}^{-1} = \mathbf{B}_m^{-1} + \frac{\boldsymbol{\gamma}_m \boldsymbol{\gamma}_m^T}{\boldsymbol{\gamma}_m^T \boldsymbol{\delta}_m} - \frac{\mathbf{B}_m^{-1} \boldsymbol{\delta}_m \boldsymbol{\delta}_m^T \mathbf{B}_m^{-1}}{\boldsymbol{\delta}_m^T \mathbf{B}_m^{-1} \boldsymbol{\delta}_m},$$

Then the diagonal elements are updated by

$$\mathbf{B}_{m+1} = \left(\frac{1}{\mathbf{B}_m} + \frac{(\boldsymbol{\gamma}_m)^2}{\boldsymbol{\gamma}_m^T \boldsymbol{\delta}_m} - \frac{(\boldsymbol{\delta}_m)^2}{(\mathbf{B}_m)^2 (\boldsymbol{\delta}_m^T \mathbf{B}_m^{-1} \boldsymbol{\delta}_m)} \right)^{-1} \quad (14)$$

The diagonal elements in \mathbf{B}_0 are initialized with positive values to ensure \mathbf{B}_0 is *positive-definite*. By (14) the computational and storage complexity of \mathbf{B} is reduced to $O(M)$.

As \mathbf{B} in DQN is a diagonal matrix, when $L(\mathbf{w})$ converges to the minimum, the diagonal elements of \mathbf{B} and \mathbf{w} are repeatedly employed to update the ARD regularization parameters as

$$\alpha_k^{new} = \begin{cases} \frac{1 - \alpha_k B_{kk}}{\hat{w}_k^2}, & \text{when } 1 - \alpha_k B_{kk} > 0 \\ \frac{c}{\hat{w}_k^2} & \text{otherwise} \end{cases} \quad (15)$$

During the iteration, there might exist a small subset of elements $1 - \alpha_k B_{kk}$ tuned smaller than 0, which violates the distribution in (3). This usually occurs when using the Gaussian kernel function with a small radius σ in the RVM framework. As small σ narrows the differentiation of the transformed feature in the kernel space, resulting in weak convergence. As α_k in SBL plays the role of governing the complexity of the corresponding w_k and truncates small $|w_k|$ when $\alpha_k \rightarrow \infty$. The accuracy usually mildly deteriorates with the truncation of w_k [5, 6]. Therefore, we utilize a small constant c as replacement of $1 - \alpha_k B_{kk}$ in (15) for such cases. This is equivalent to preventing the truncation of the associated w_k and retaining for updating in the subsequent iteration, with a little sacrifice of sparsity without loss of accuracy. For those very small $|\hat{w}_k|$, α_k^{new} is guaranteed to be updated to a large value using $\frac{c}{\hat{w}_k^2}$ and might result to truncate the associated $|\hat{w}_k|$, in turn.

It only contains element-wise floating computation in formula (15), whose complexity is $O(M)$. Using (14), the Storage and calculation of the full inverse Hessian matrix is ignored but replaced by a diagonal matrix \mathbf{B} using $\boldsymbol{\delta}_m$ and $\boldsymbol{\gamma}_m$ in all iterations. The complexity is therefore reduced from $O(M^3)$ in the classical SBL to $O(M)$ in our algorithm, making it scale well to large-scale problems. We name this algorithm DQN-SBL in this paper.

C. Summary of DQN

DQN is summarized in **Algorithm 1**. In our implementation, some settings are noted below.

1) \mathbf{B} is initialized with an identity diagonal matrix and updated with Step 10 at **Algorithm 1**, by which \mathbf{B} is guaranteed to be *positive definite* in the following iterations. Once the gradient $\nabla L(\mathbf{w}_m)$ falls below a given tolerance ε , a stable \mathbf{B} is approximated. In order to guarantee convergence, a maximum number of iterations *MaxIts_qn* is predefined.

2) The step size η (Step 5, **Algorithm 1**) is normally determined by a line search algorithm that satisfies the wolf

condition [20]. Variations of line search methods may result to different convergence speeds. In this paper, we do not describe the details about the line search methods [23]. The direction \mathbf{p}_m here is scaled before imported to *linesearch* in step 5 to accelerate the learning speed.

Algorithm 1 DQN method $[\mathbf{w}, \mathbf{B}] = \text{DQN}(\mathbf{X}, \mathbf{t}, \mathbf{w}, \boldsymbol{\alpha})$

Given objective function $L(\mathbf{w})$ and its gradient $\nabla L(\mathbf{w})$ function;

Initialize output weights vector \mathbf{w} ;

Convergence tolerance $\varepsilon > 0$, maximum iteration *MaxIts_qn*;

1 iteration $m \leftarrow 0$

2 $\mathbf{B}_0 = \text{diag}(\mathbf{I})$ //O(M)

While $\|\nabla l(\mathbf{w})\| > \varepsilon$ && $m < \text{MaxIts_qn}$

3 $\mathbf{p}_m = -\mathbf{B}_m \cdot \nabla L(\mathbf{w}_m)$

4 $\mathbf{p}_m = \mathbf{p}_m / \|\mathbf{p}_m\|$ //accelerate convergence

5 $\eta_m = \text{linesearch}(\mathbf{w}_m, \mathbf{p}_m)$

6 $\boldsymbol{\delta}_m = \eta_m \mathbf{p}_m$

7 $\mathbf{w}_{m+1} = \mathbf{w}_m + \boldsymbol{\delta}_m$

8 $\boldsymbol{\gamma}_m = \nabla L(\mathbf{w}_{m+1}) - \nabla L(\mathbf{w}_m)$

9 calculate \mathbf{B}_m with (14)

10 $m \leftarrow m + 1$

12. return \mathbf{w}_m and \mathbf{B}_m

Once the convergence criterion of \mathbf{w} in **Algorithm 1** is met, the approximated \mathbf{B}_m plays the role of inverse Hessian matrix $\boldsymbol{\Sigma}$ and is employed to update the hyperparameters $\boldsymbol{\alpha}$.

D. Summary of DQN-SBL

The algorithm of DQN-SBL for classification is summarized in **Algorithm 2**, in which it mainly contains two stages: estimation of output weights \mathbf{w} at **MAP-stage**; updating regularization hyperparameters $\boldsymbol{\alpha}$ at **A-stage**. These two stages are repeatedly conducted until the termination condition is satisfied.

MAP-stage: The weight \mathbf{w} is estimated and the inverse Hessian matrix \mathbf{B} is calculated. The step size η is usually obtained by the line search method, which satisfies the wolf-condition.

A-stage: Updating the regularizations parameters $\boldsymbol{\alpha}$ using the convergent $\hat{\mathbf{w}}$ and \mathbf{B} from the **MAP-stage**. For those α_k , it tends to grow infinity (greater than a very large value here), pruning the associated w_k (set zero here) and will not be updated in the subsequent iteration. Analogous to SBL, once the convergence is reached at **MAP-Stage**, \mathbf{w} and \mathbf{B} are taken to update $\boldsymbol{\alpha}$.

E. Complexity analysis of DQN-SBL

In SBL, the largest complexity consumption is the calculation of the Hessian matrix inversion at the **MAP-Stage**, which takes $O(M^3)$ computational complexity and $O(M^2)$ storage memory. While in DQN-SBL, this inversion is replaced by (14). The memory for storages and calculation of \mathbf{B} , $\boldsymbol{\delta}$ and $\boldsymbol{\gamma}$ are $O(M)$.

Therefore, DQN-SBL scales well to high-dimensional problems (or large N in RVMs).

method [11] to decompose the multiclass classification into binary problems and then ensemble for final prediction in our experiments.

Algorithm 2: Summary of DQN-SBL

Initialization:

Given dataset $\mathcal{D} = (\mathbf{x}_i, \mathbf{t}_i)$, $i = 1$ to N .
 Given *MaxIts*, *ALPHA_MAX*, *DELTA_LOGALPHA*, a small *init_alpha*, *c*
 $\mathbf{w} = [\mathbf{0}]_{L \times 1}$, $\alpha = \text{init_alpha} * [1]_{L \times 1}$

MAP-Stage: conducting weights \mathbf{w} and the inverse Hessian matrix \mathbf{B}

1. $[\mathbf{w}, \mathbf{B}] = \text{DQN}(\mathbf{X}, \mathbf{t}, \mathbf{w}, \alpha)$

A-Stage: Estimation of hyperparameters α .

2. For every α_k ,
 Update α_k using (15)
 End for

3. For every α_k in α ,
 If $\alpha_k > \text{ALPHA_MAX}$ //i.e., $\alpha_k \rightarrow \infty$
 prune α_k and the associated \mathbf{w}_k ;
 End if
 End for

4. If the largest absolute difference between two successive logarithmic values of α_k is lower than the *given* tolerance *DELTA_LOGALPHA*, then stop. Otherwise, repeat the **MAP-Stage** and **A-Stage** until the maximum iteration *MaxIts*.

1) *Experimental Setup*

There are 19 benchmarks in our experiments. The properties of the experimental datasets are listed in Table I. The datasets were downloaded from the Libsvm machine learning repository [24], where the dataset has been fetched from other well-known machine repositories and preprocessed beforehand. The first 15 benchmarks with relatively small training data size or feature size are used for evaluation on DQN-RVM, RVM, DQN-SBELM and SBELM. All features of these 15 datasets are linearly scaled to $[-1, 1]$. The last four benchmarks with large-scale discrete feature size and training data are selected to evaluate the linear DQN-SBL on feature selection and classification. Some settings for experiments are listed belows:

- a) In our implementation, we keep most settings the same for each group of experiments. Except that SBL is employed to RVM and SBELM, DQN-SBL to DQN-RVM and DQN-SBELM at **W-Stage** respectively. we set *DELTA_LOGALPHA* = 10^{-3} , *ALPHA_MAX* = 10^6 , *MaxIts* = 100, *c*=0.0001 for **Algorithm 2** and $\epsilon = 10^{-1}$, *MaxIts_qn* = 100 for **Algorithm 1**.
- b) We implement the 4 algorithms based on the open-source toolboxes SBELM_v1.1 [25]. The activation function for DQN-SBELM, and SBELM for the hidden layer is sigmoid $\sigma(\mathbf{a}, b, x) = 1/(1 + \exp(-(\mathbf{a}x + b)))$, where \mathbf{a}, b are the random generated synapses and bias with uniform distribution within $[-1, 1]$ respectively.

IV. EXPERIMENTAL EVALUATION

A. *DQN-SBL for Non-linear Classification*

In this section, we conduct experiments to verify the effectiveness of DQN-SBL in non-linear classification (integrated into RVM). For a thorough evaluation, we also integrate DQN-SBL into SBELM and compared with its original counterpart. SBELM [11] is a three-layer (input-hidden-output) feedforward network that randomly maps the raw feature into a larger number of hidden nodes L and employs SBL to select the most relevant hidden nodes, achieving competitive accuracy and sparsity. SBELM resolves the drawback of RVM in handling problems with large scale training instances N with much lower computational complexity $O(L^3)$, compared to $O(N^3)$ in RVM when $L \ll N$. One may refer to the work [11] for more details.

Two groups of experiments are conducted: RVMs (DQN-RVM, RVM) and SBELMs (DQN-SBELM, SBELM). RVMs and SBELMs transform raw features to kernel space and random layer respectively. The transforming method inner each group of experiments is the same. A brief summary,

DQN-RVM: integrating DQN-SBL into RVM

DQN-SBELM: integrating DQN-SBL into SBELM

At first, these four algorithms are evaluated on a variety of benchmarks with a relatively small dataset. Secondly, DQN-SBL for feature selection is evaluated on several large-scale datasets with large training data size and high dimensional feature space.

As DQN-SBL and SBL are originally proposed for binary classifications, we utilize the pairwise coupling (one-vs-one)

TABLE I
PROPERTIES OF TRAINING DATASET

Dataset	Instances	Features	Classes
Adult1	1605	124	2
colon	62	2001	2
breast	683	11	2
diabetes	768	9	2
german_numer	1000	25	2
a2a	2265	121	2
madelon	600	502	2
usps.binary	2199	258	2
Iris	150	5	3
Wine	178	14	3
segment	2310	20	7
satimage	4435	37	6
usps.all	7291	258	10
news20	19304	1355191	2
real-sim	71362	20958	2
rcv1.binary.train	19663	47236	2
url_combined	515006	3231961	2

- c) A 5-fold cross-validation strategy is used for evaluating the performance. We compare the mean validation accuracy, sparsity, and training time under the best hyperparameters. For RVMs, the kernel radius hyperparameter σ is searched in $2^{[-5,5]}$.
- d) For SBELMs, the number of hidden neurons and the seed s for generating random hidden synapses and bias $[L, s]$ are

>SPARSE BAYESIAN CLASSIFICATION WITH DIAGONAL QUASI-NEWTON METHOD FOR LARGE SCALE LEARNING<

taken from the grid search by $[50, 100, 150, 200] \times [1, 2, 3, 4, 5]$ e) To collect more binary datasets, the benchmark *usps.binary* is for small feature size problems (<100), and $[100, 500, 900, 1300] \times [1, 2, 3, 4, 5]$ for others. In general, the accuracy for SBELM under different s for generating random weights are with minor difference. f) All experiments analyzed in this subsection are run on a 3.60GHz-CPU with 16-GB RAM PC.

TABLE II
COMPARISON OF ACCURACY

Dataset	DQN-RVM	RVM	DQN-SBELM	SBELM
Adult1	75.39±0	75.39±0	75.39±0	75.39±0
colon	77.86±8.4	79.52±8.52	85.95±10.66	76.19±11.45
breast	96.94±1.47	97.35±1.26	96.91±1.35	96.78±0.97
diabetes	75.91±1.72	78.13±1.05	76.31±2.08	78.26±2.05
german	75.3±3.47	76.7±3.44	76.6±3.45	76.6±3.93
a2a	81.64±2.31	81.86±2.11	81.95±2.15	81.33±2.61
madelon	65.33±3.56	65±4.29	58±3.04	58.83±4.19
<i>usps.binary</i>	99.82±0.19	99.91±0.12	99.73±0.1	99.73±0.1
Iris	95.33±3.8	96.67±3.33	97.33±2.79	97.33±4.35
Wine	96.58±2.51	98.35±2.58	97.06±5.09	97.87±2.94
segment	94.55±0.1	96.62±0.86	95.76±0.85	96.97±0.59
satimage	89.49±1.38	90.78±1.17	86.45±1.83	88.86±1.26
usps.all	95.39±0.7	96.63±0.83	95.45±0.69	-

'-' denotes suffering ill-conditional issue.

TABLE III
COMPARISON OF SPARSITY

Dataset	DQN-RVM	RVM	DQN-SBELM	SBELM
Adult1	4.00	47.00	6.00	7.00
colon	6.60	7.00	22.00	9.00
breast	4.00	5.00	4.00	7.00
diabetes	125.00	8.00	4.00	10.00
german	190.20	11.00	10.00	15.00
a2a	383.00	20.00	47.00	94.00
madelon	480.00	480.00	49.00	85.00
<i>usps.binary</i>	8.40	5.00	7.00	7.00
Iris	3.67×3	4.00×3	3.67×3	4.00×3
Wine	3.67×3	5.33×3	3.00×3	4.33×3
segment	32.81×21	5.43×21	4.43×21	5.38×21
satimage	131.80×15	15.00×15	6.67×15	12.73×15
usps.all	119.69×45	8.25×45	45.24×45	-

'-' denotes suffering ill-conditional issue.

We roughly measure the sparsity for the trained model using the number of the remaining basis functions and hidden nodes in RVMs and SBELMs. \times denotes multiplying the number of binary classifiers using the one-vs-one training strategy

>SPARSE BAYESIAN CLASSIFICATION WITH DIAGONAL QUASI-NEWTON METHOD FOR LARGE SCALE LEARNING<

TABLE IV
COMPARISON OF TRAINING TIME(SECONDS)

Dataset	DQN-RVM	RVM	DQN-SBELM	SBELM
Adult1	1.88E+03	5.62E+02	4.84E+02	2.51E+02
colon	8.03E+01	1.08E+01	3.30E+02	1.48E+02
breast	5.38E+02	2.30E+02	8.86E+01	6.77E+00
diabetes	4.30E+02	1.23E+02	5.05E+01	5.58E+00
german	7.44E+02	2.21E+02	1.34E+02	2.03E+02
a2a	4.38E+03	1.29E+03	1.34E+03	3.31E+02
madelon	2.06E+02	3.01E+02	3.23E+02	1.53E+02
usps.binary	6.32E+03	3.14E+03	3.93E+02	1.63E+01
Iris	8.10E+02	5.34E+01	2.37E+02	7.14E+00
Wine	2.31E+02	5.99E+01	2.34E+02	1.46E+01
segment	4.36E+04	2.87E+03	1.62E+03	1.20E+02
satimage	2.44E+04	1.75E+04	2.06E+03	1.87E+02
usps.all	8.63E+04	2.16E+04	4.20E+04	-

‘-’ denotes suffering ill-conditional issue

TABLE V
COMPARISON OF COMPLEXITIES

Dataset	DQN-RVM / RVM (Ratio)		DQN-SBELM / SBELM (Ratio)	
	Computational Complexity	Storage Complexity	Computational Complexity	Storage Complexity
Adult1	3.88E-07	6.23E-04	5.92E-07	7.69E-04
colon	2.60E-04	1.61E-02	5.92E-07	7.69E-04
breast	2.14E-06	1.46E-03	2.50E-05	5.00E-03
diabetes	1.70E-06	1.30E-03	2.50E-05	5.00E-03
german	1.00E-06	1.00E-03	2.50E-05	5.00E-03
a2a	1.95E-07	4.42E-04	5.92E-07	7.69E-04
madelon	2.78E-06	1.67E-03	5.92E-07	7.69E-04
usps.binary	2.07E-07	4.55E-04	5.92E-07	7.69E-04
Iris	4.44E-05	6.67E-03	2.50E-05	5.00E-03
Wine	3.16E-05	5.62E-03	2.50E-05	5.00E-03
segment	1.87E-07	4.33E-04	2.50E-05	5.00E-03
satimage	5.08E-08	2.25E-04	2.50E-05	5.00E-03
usps.all	1.88E-08	1.37E-04	5.92E-07	7.69E-04

‘-’ denotes suffering ill-conditional issue

2) Comparison of Accuracy

The comparison of best accuracies on these benchmarks are listed in Table II. The marginal decisive probabilistic score for all classifiers is set to 0.5. Overall, SBELMs (DQN-SBELM, SBELM) are a little better than RVMs (DQN-RVM, RVM). We here separately analyze them. The accuracies of the RVMs and

SBELMs are very close in most benchmarks except that DQN-SBELM is much higher than others in *colon* (feature size > 3000 and > 7000 respectively), this may verify that DQN-SBL is more robust to the problems with high-dimensional problems. Meanwhile, SBELM is stuck into the ill-conditioning issue on *usps.all* in our hyperparameter search scope.

>SPARSE BAYESIAN CLASSIFICATION WITH DIAGONAL QUASI-NEWTON METHOD FOR LARGE SCALE LEARNING<

Furthermore, in order to compare the stability under different parameter settings. We depict the accuracy under different hyperparameters (σ) for RVMs and SBELMs in Figs. 1 and Figs. 2, respectively. The accuracy curves for DQN-RVM and RVM are very close in most of benchmarks under different σ , except with small fluctuation in *colon-2000*, *diabetes* and *madelon*. But the two models can achieve close best accuracy under the parameter selection scope for this 3 benchmarks. The accuracy curves of SBELMs is much stable under different L , as shown in Fig.2. Nevertheless, it achieves competitive accuracy amongst most datasets. This verifies the aim of our work: *the same accuracy and sparsity but with lower computational and storage complexity*.

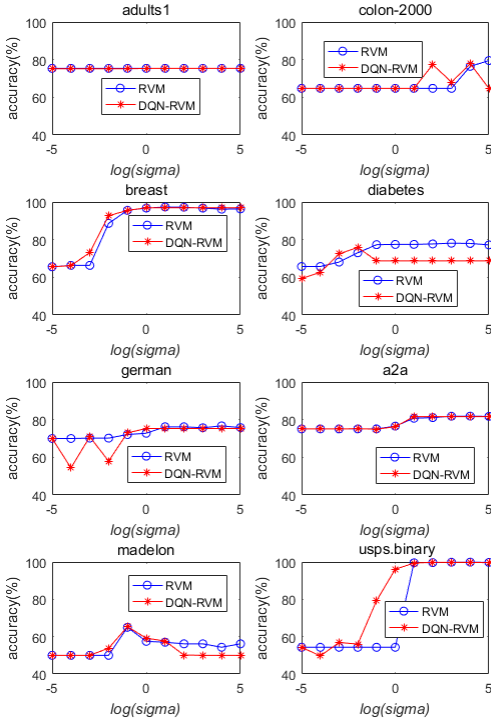


Fig. 1. Accuracy of RVMs under different hyperparameter ($\log \sigma$)

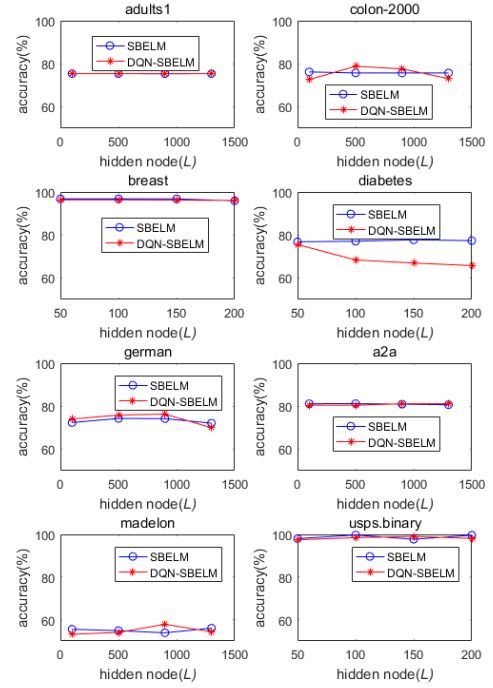


Fig. 2. Accuracy of SBELMs under different number of hidden nodes (L).

3) Comparison of Sparsity

we measured the sparsity using the average size of the remaining number of basis functions for RVMs and the remaining hidden nodes (L_{remain}) for SBELMs. Table III records the sparsity values corresponding to the best accuracy in Table II. Overall, the sparsity in SBELMs is of the same magnitude. The sparsities for the RVMs are very close, while for some benchmarks DQN-RVM performs quite fluctuating. Look at to Fig. 1, RVMs perform better at large σ where the sparsities are smaller and the accuracies are better. However, the sparsity of DQN-RVM is much smaller than the training data size, and its corresponding accuracy in Table II is close to the original RVM. In practical applications with large-scale training data, RVM is not a preferable choice, but DQN-RVM tackles this obstacle well.

In addition to evaluating the sparsity. We also depict the sparsity under different σ and L on the first 8 datasets for RVMs and SBELMs in Fig. 3 and Fig. 4 respectively. Overall speaking, RVM is sparser than DQN-RVM at small σ in Figs. 3. The reason is that there might exist a small subset of $1 - \alpha_k B_{kk} < 0$ during the training and α_k^{new} is updated by $\frac{c}{\tilde{w}_k^2}$, the truncation for some small $|w_k|$ is prevented, Nevertheless, the accuracy is not affected but close to the RVM algorithm, as shown in Fig. 1. This phenomenon alleviates to the same level with other algorithms at larger σ where the best accuracy is usually achieved under, which verifies our previous analysis in Section III.B.

>SPARSE BAYESIAN CLASSIFICATION WITH DIAGONAL QUASI-NEWTON METHOD FOR LARGE SCALE LEARNING<

The sparsity of DQN-SBELM is sparser than SBELM under different L in Fig. 4 and keep stable with increasing of L in both DQN-SBELM and SBELM. The accuracy of this two models under different L is quite stable.

The sparsities of SBELMs on most datasets are very close and stable. For the DQN based models, the sparsity of DQN-SBELM is much smaller than DQN-RVM. This implies that DQN-SBL works better on the random-mapping feature space than the Gaussian kernel space. The sparsity on the Gaussian kernel method is sensitive to the hyperparameter. Therefore, when number of training instances increases, SBELM is usually more preferable than RVM with lower computational complexity, as analyzed in work [11].

4) Comparison of Training time and complexity

We evaluate the training time starting from the grid-search until the completion of the training process for each benchmark. The training time is recorded in Table IV. The training times in the RVMs are very close to each other under the same magnitude while DQN-SBELM takes much longer time than SBELM on several datasets. Nevertheless, the two SBELMs model can finish training within an hour as it contains 4 *hidden nodes* \times 5 *seeds* = 20 grid-search trials and can finish in minutes for a search. As shown in Fig. 2, the accuracy of SBELM is insensitive to the number of hidden nodes and seed in these two models. Practically the training time can be further shortened by reducing the grid search scope. Moreover, in most application scenarios, training time is not the main concern but the execution time with an accurate and sparse model.

Apart from comparing the training time, we add one more comparison on the computation and storage complexity of our proposed models versus the base line models. As most of settings inner the RVMs and SBELMs are kept same. Therefore, we mainly have a sight on the ratio of our proposed models over the base line models. We roughly define

$$\text{computation_complexity_ratio}(\text{DQN-SBELM} / \text{SBELM}) = \frac{O(L)}{O(L^3)} = 1/(\max(L))^2$$

$$\text{computation_complexity_ratio}(\text{DQN-RVM} / \text{RVM}) = \frac{O(N)}{O(N^3)} = 1/N^2$$

$$\text{storage_complexity_ratio}(\text{DQN-SBELM} / \text{SBELM}) = \frac{O(L)}{O(L^2)} = 1/\max(L)$$

$$\text{storage_complexity_ratio}(\text{DQN-RVM} / \text{RVM}) = \frac{O(N)}{O(N^2)} = 1/N$$

The complexity ratios are listed in Table V. The average computation and storage complexity ratio of DQN-RVM / RVM are on 1E-6 and 1E-3 respectively. This exponentially increases by the number of training data N . We can imagine that when N is large enough, it will result to the memory-overflow issue and consume longer training time in the RVM. On the other hand, the average computation and storage complexity of DQN-SBELM / SBELM are about 1E-6 and 1E-3 respectively.

As a larger number of hidden nodes than the feature dimension is required for the SBELMs model to enable better generalization. When the feature dimension increases, it will also result to the memory-issue and consume longer training time in SBELM model.

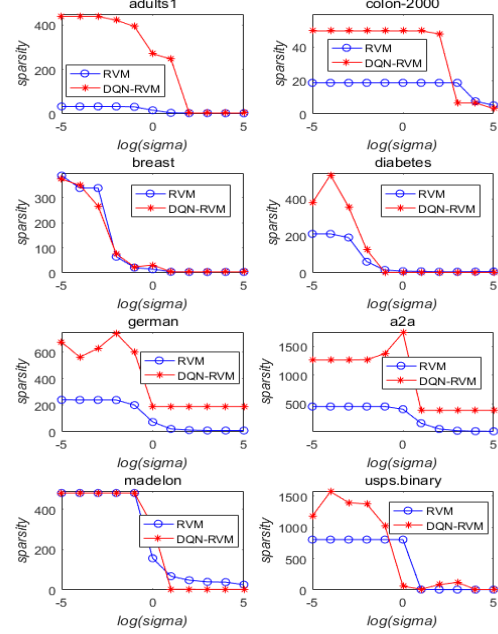


Fig. 3. Sparsity of RVMs under different hyperparameter ($\log \sigma$)

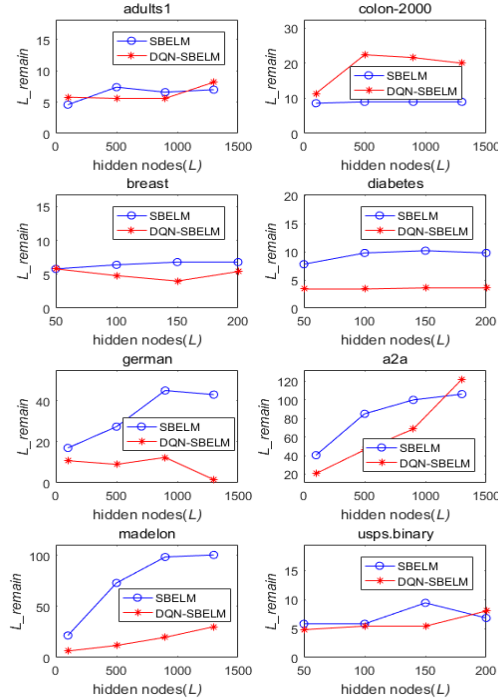


Fig. 4. Sparsity of SBELMs under different number of hidden nodes (L).

>SPARSE BAYESIAN CLASSIFICATION WITH DIAGONAL QUASI-NEWTON METHOD FOR LARGE SCALE
LEARNING<

In a nutshell, DQN-RVM is with same or analogous accuracy and training time compared with RVM. Although the sparsity of DQN-RVM is relatively higher in several benchmarks, the model size is still very small and the computational complexity are $O(N)$, compared to the $O(N^3)$ in RVM. DQN-RVM is scalable to large problems with large training data size N . Meanwhile, DQN-SBELM inherits the advantages of SBELM in achieving a very sparse model and high generalization but with mildly longer training time. While the computational complexities of DQN-SBELM is $O(L)$ compared to $O(L^3)$ in SBELM. When the feature dimension increases, a much larger L is required to enable competitive generalization, but a large L may result in the memory-overflow in SBELM. While DQN-SBELM can avoid this issue. Most importantly, both DQN-RVM and DQN-SBELM overcome the harsh memory requirement of RVM and SBELM for large problems, which meets the research objective of our proposed DQN-SBL.

B. DQN-SBL for Feature Selection

1) Experimental Setup

This section focuses on evaluating DQN-SBL on large-scale linear classifications with very high dimensional feature space where memory overflow may arise using SBL for such applications. Previous work on using SBL for feature selection is mainly on small problems in the literature. Four benchmarks *news20*, *real-sim*, *rcv1.binary.train* and *url_combined* on document classification are selected in our experiment, as listed in Table IV. Each dataset is randomly split into $\frac{3}{4}$ for training data and $\frac{1}{4}$ for test data.

DQN-SBL is compared with the l_2 -norm logistic regression (LR-12). Like DQN-SBL, LR-12 has the analogous log-likelihood function, that utilizes a unified regularization parameter λ to control the complexity of \mathbf{w} . While in SBL, the unified λ is replaced with a series of α_k ($k = 0, \dots, M$) to independently govern each w_k . In DQN-SBL, each α_k is automatically determined from the training data while the best λ in LR-12 is achieved by an exhaustive cross-validation.

TABLE V
COMPARISON OF ACCURACY

Dataset	DQN-SBL	LR-12
<i>news20</i>	96.85	97.06
<i>real-sim</i>	97.25	97.34
<i>rcv1.binary.train</i>	96.50	96.72
<i>url_combined</i>	98.54	97.89

2) Accuracy

As SBL and its variants provide a trade-off between the sparsity and accuracy, its accuracy may mildly deteriorate to be underfitting with increasing iterations at **A-stage** in some problems. Therefore, in terms of best accuracy, we conduct the experiments without consideration of sparsity for DQN-SBL. An extra 5-fold cross-validation strategy is employed for DQN-SBL to search the ‘early-stopping’ iteration *iter* with best validation accuracy. After that, we train a new classifier terminated at the *iter* for predicting the test dataset. For the best

hyper-parameter λ in LR-12, it is also achieved by a 5-fold cross-validation at scope $\lambda \in 2^{[-5,5]}$ with increasing step size by 2.

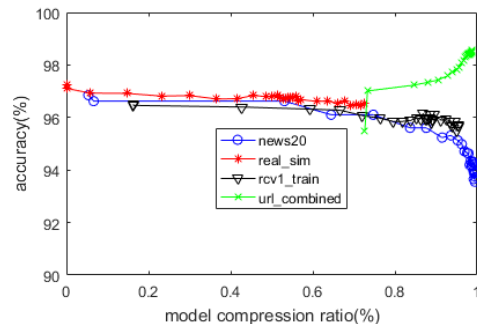


Fig. 5 Accuracy under different feature ratio, here define ratio= $1 - \text{size}(\mathbf{w}^{\neq 0})/M$.

The accuracy of these two models is listed in Table V. It is easy to conclude that the best accuracies of the two models are very close. However, the best results on LR-12 are obtained by exhaustive cross-validations, which may become a burden for large-scale problems in finding the best λ because it is very time-consuming for repeatedly loading data to memory in search of λ . DQN-SBL avoids the hyper-parameters selection as the α are automatically learned in the training phase.

3) Model Compression

The generalization does not sharply deteriorate with the higher sparsity. To verify this assumption, we draw the evolution curves of the accuracies on the four datasets at different sparsity levels in Fig. 5. The accuracies in *news20*, *real-sim*, *rcv1.binary.train* mildly decrease with the increasing sparsity except *url_combined* performs inversely, where the remaining feature size decreases, while the accuracy increases.

V. DISCUSSION

As the severe complexity in SBL mainly focus on calculating the covariance matrix in the MAP function. While it is essential to update the regularization parameter using this inverted matrix. In this paper, DQN-SBL is proposed by using a diagonal quasi-newton method for the **MAP** where the calculation of the covariance matrix is ignored but approximated by a diagonal matrix \mathbf{B} and iteratively updated using the differences of \mathbf{w} and the gradients $\nabla L(\mathbf{w})$. Once converged, the diagonal elements of \mathbf{B} are employed to update the regularization α alternately. The storage and computational complexity of \mathbf{B} using (13) are $O(M)$ in DQN-SBL ($O(N)$ in DQN-RVM, $O(L)$ in DQN-SBELM). The complexity of the matrix inversion in SBL with $O(M^3)$ is shorten to $O(M)$ in DQN-SBL. It is especially well suitable for large problems. The complexities are listed in the following Table VI.

Strictly speaking, the datasets on evaluating DQN-SBL is not the truly large-scale data that can't be loaded into memory or processed by available computation resources. The experiments conducted in this paper aim to verify that DQN-SBL is with analogous accuracy and sparsity to SBL, but with linear complexity $O(M)$ to scale well for large scale problems. The experiment results described above verify this conclusion.

TABLE VI
COMPLEXITY OF SBL VARIANTS

Model	Computation complexity	Storage complexity
SBL	$O(M^3)$	$O(M^2)$
DQB-SBL	$O(M)$	$O(M)$
RVM	$O(N^3)$	$O(N^2)$
DQN-RVM	$O(N)$	$O(N)$
SBELM	$O(L^3)$	$O(L^2)$
DQN-SBELM	$O(L)$	$O(L)$

M : feature dimension. N : number of training data. L : number of hidden nodes in SBELMs.

VI. CONCLUSION

This paper extends the efficient learning technique SBL for large-scale learning by developing a diagonal Quasi-newton method (DQN-SBL) for its MAP function. The new method overcomes the limitation of SBL that requires a memory-intensive covariance matrix inversion with complexity $O(M^3)$ (M : feature size) in the MAP to alternately update the regularized parameters. In DQN-SBL, the matrix inversion is approximated by a positive diagonal matrix and iteratively updated using the previous \mathbf{w} and gradients. In this way, the computational complexity and storage memory are both reduced to $O(M)$ and therefore DQN-SBL scales well to large-scale problems.

Based on DQN-SBL, DQN-RVM and DQN-SBELM are proposed in this paper. DQN-RVM is proposed to overcome the complexity $O(N^3)$ (N : training data size) of RVM for basis selection and achieves analogous accuracy and sparsity to RVM, but with complexity $O(N)$. Similarly, DQN-SBELM reduces the complexity of SBELM from $O(L^3)$ to $O(L)$ (L : num of hidden nodes) for high dimensional problems. As a summary, DQN-SBL is very suitable for large-scale problems, where no exhaustive regularized parameter selection is required in DQN-SBL. We also verify the advantage of DQN-SBL on large scale linear feature selection problems in our experiment, it achieves competitive accuracy with extremely small model size.

VII. REFERENCE

- [1] J. Liu, J. Chen, and J. Ye, "Large-scale sparse logistic regression," in *Proceedings of the 15th ACM SIGKDD international conference on Knowledge discovery and data mining*, 2009, pp. 547-556.
- [2] H. B. McMahan, "Follow-the-regularized-leader and mirror descent: Equivalence theorems and ℓ_1 regularization," 2011.
- [3] C. Cortes, V. Vapnik, "Support-Vector Networks," *Machine Learning*, vol. 20, no. 3, pp. 273-297, 1995.
- [4] T. Joachims, "Making Large-Scale Support Vector Machine Learning Practical," *Advances in kernel methods*, pp. 169-184: MIT press, 1999.
- [5] M. E. Tipping, "Sparse Bayesian learning and the relevance vector machine," *Journal of Machine Learning Research*, vol. 1, pp. 211-244, Sum 2001.
- [6] A. C. Faul, M. E. Tipping, "Analysis of Sparse Bayesian Learning," *Advances in Neural Information Processing Systems*, pp. 383-390: MIT Press, 2002.
- [7] Z. L. Zhang and B. D. Rao, "Extension of SBL Algorithms for the Recovery of Block Sparse Signals With Intra-Block Correlation," *IEEE Transactions on Signal Processing*, vol. 61, pp. 2009-2015, Apr 2013.
- [8] M. Al-Shoukairi, P. Schniter, and B. D. Rao, "A GAMP-based low complexity sparse Bayesian learning algorithm," *IEEE Transactions on Signal Processing*, vol. 66, pp. 294-308, 2017.
- [9] B. Worley, "Scalable Mean-Field Sparse Bayesian Learning," *IEEE Transactions on Signal Processing*, vol. 67, pp. 6314-6326, 2019.
- [10] H. Duan, L. Yang, J. Fang, and H. Li, "Fast inverse-free sparse bayesian learning via relaxed evidence lower bound maximization," *IEEE Signal Processing Letters*, vol. 24, pp. 774-778, 2017.
- [11] J. H. Luo, C. M. Wong, P. K. Wong, "Sparse Bayesian Extreme Learning Machine for Multi-classification," *IEEE transactions on neural networks and learning systems*, vol. 25, no. 4, pp. 836-843, 2014.
- [12] J. H. Luo, C. M. Wong, and C. M. Wong, "Multinomial Bayesian extreme learning machine for sparse and accurate classification model," *Neurocomputing*, vol. 423, pp. 24-33, Jan 2021.
- [13] C. M. Bishop and M. E. Tipping, "Variational relevance vector machines," in *Proceedings of the Sixteenth conference on Uncertainty in artificial intelligence*, 2000, pp. 46-53.
- [14] M. J. Beal, *Variational Algorithms for Approximate Bayesian Inference*. University of London, London, 2003.
- [15] Y. Mohsenzadeh, H. Sheikhzadeh, A. M. Reza, N. Bathaee, and M. M. Kalayeh, "The Relevance Sample-Feature Machine: A Sparse Bayesian Learning Approach to Joint Feature-Sample Selection," *IEEE Transactions on Cybernetics*, vol. 43, pp. 2241-2254, Dec 2013.
- [16] Y. Mohsenzadeh and H. Sheikhzadeh, "Gaussian Kernel Width Optimization for Sparse Bayesian Learning," *IEEE Transactions on Neural Networks and Learning Systems*, vol. 26, pp. 709-719, Apr 2015.
- [17] I. Psorakis, T. Damoulas, and M. A. Girolami, "Multiclass relevance vector machines: Sparsity and accuracy," *IEEE Transactions on Neural Networks*, vol. 21, no. 10, pp. 1588-1598, Oct. 2010.
- [18] S. Lyu, X. Tian, Y. Li, B. Jiang, H. Chen, "Multiclass probabilistic classification vector machine," *IEEE Transactions on Neural Networks*, vol. 31, no. 10, pp. 3906 - 3919, Oct. 2020
- [19] H. Chen, P. Tino, and X. Yao, "Efficient Probabilistic Classification Vector Machine With Incremental Basis Function Selection," *IEEE Transactions on Neural Networks*, vol. 25, no. 2, pp. 356- 369, Feb. 2014.
- [20] D. C. Liu, J. Nocedal, "On the Limited Memory BFGS Method for Large Scale Optimization," *Mathematical Programming*, vol. 45, no. 1-3, pp. 503-528, 1989.

>SPARSE BAYESIAN CLASSIFICATION WITH DIAGONAL QUASI-NEWTON METHOD FOR LARGE SCALE
LEARNING<

- [21] J. E. Dennis, H. Wolkowicz, "Sizing and least-change secant methods ". *SIAM. J. Numer. Anal.* 30, pp.1291–1314, 1993
- [22] S. Saarinen, R. Bramley, G. Cybenko, "Ill-Conditioning in Neural Network Training Problems," *SIAM Journal on Scientific Computing*, vol. 14, no. 3, pp. 693-714, 1993.
- [23] D. F. Shanno, "Conditioning of Quasi-Newton Methods for Function Minimization," *Mathematics of computation*, vol. 24, no. 111, pp. 647-656, 1970.
- [24] <http://www.csie.ntu.edu.tw/~cjlin/libsvmtools/datasets/>
- [25] <http://www.fst.umac.mo/en/staff/documents/fstcmv/SBELM%20Classification%20V1.1.zip>
- [26] A. Mokhtari and A. Ribeiro, "A quasi-newton method for large scale support vector machines," in *2014 IEEE International Conference on Acoustics, Speech and Signal Processing (ICASSP)*, 2014, pp. 8302-8306.
- [27] C.J. Lin, R.C. Weng and S. S. Keerthi, "Trust Region Newton Method for Large-Scale Logistic Regression," in *Journal of Machine Learning Research*, 2008, pp. 627-650.
- [28] W. Chen, " Simultaneously Sparse and Low-Rank Matrix Reconstruction via Nonconvex and Nonseparable Regularization," *IEEE Transactions on Signal Processing*, vol. 66, pp. 5313-5323, Sep 2018